The effect of "pre-formed" hadron potentials on the dynamics of heavy ion collisions and the HBT puzzle

Qingfeng Li,[1*] Marcus Bleicher,[2] and Horst Stöcker[1,2,3]
1) Frankfurt Institute for Advanced Studies (FIAS), Johann Wolfgang Goethe-Universität, Max-von-Laue-Str. 1, D-60438 Frankfurt am Main, Germany
2) Institut für Theoretische Physik, Johann Wolfgang Goethe-Universität, Max-von-Laue-Str. 1, D-60438 Frankfurt am Main, Germany
3) Gesellschaft für Schwerionenforschung, Darmstadt (GSI), Germany

The nuclear stopping, the elliptic flow, and the HBT interferometry are calculated by the UrQMD transport model, in which potentials for "pre-formed" particles (string fragments) from color flux-tube fragmentation as well as for confined particles are considered. This description provides stronger pressure at the early stage and describes these observables better than the default cascade mode (where the "pre-formed" particles from string fragmentation are treated to be free-streaming). It should be stressed that the inclusion of potential interactions pushes down the calculated HBT radius R_O and pulls up the R_S so that the HBT time-related puzzle disappears throughout the energies from AGS, SPS, to RHIC.

PACS numbers: 25.75.Gz,25.75.Dw,24.10.Lx

One of the most important discoveries from SPS and RHIC experiments in the beginning of this century is that a new form of matter is produced in high energy ion collisions that seems to behave as a strongly interacting quark gluon plasma (sQGP) [1, 2, 3, 4]. Furthermore, at RHIC energies, the sQGP seems to be a nearly "perfect liquid" with small viscosity [5, 6]. Although hydrodynamical studies are a useful tool for the theoretical investigations at RHIC energies, hydrodynamics fails at lower energies. Therefore, a relativistic dynamic transport approach, in which an entire equilibrium is not pre-assumed, is necessary to explore the excitation functions of various observables. In addition, the transport model has the advantage of observing the whole phase-space evolution of all particles involved in a microscopic fashion.

In order to detect this new matter - quark gluon plasma (QGP) - many theoretical suggested observables have been discussed and argued frequently. Among these, the Hanbury-Brown-Twiss interferometry (HBT) or Femtoscopy technique has been used widely to extract the spatio-temporal information of the particle freeze-out source. It would be a vital discovery if there is an nontrivial transition in the spatio-temporal characteristics of the source, when going from low to high beam energies [7]. Experimentally, the HBT parameters have been scanned thoroughly over the energies from SIS, AGS, SPS, up to RHIC, unfortunately, no obvious discontinuities do appear [8].

However, this "null" result does not mean that the HBT technique comes to an end. Non-Gaussian effects might shadow the possible energy dependence of the HBT parameters ("*E-puzzle*"), and this topic has been quickly improving in the recent years [9, 10, 11]. Secondly, even with a Gaussian parametrization, we found that the HBT time-related puzzle ("*t-puzzle*") is present at almost all energies from AGS to RHIC [12]. In order to understand the origins of these "puzzles", it is necessary to dig deeper into the dynamics of the heavy ion collisions.

The hydrodynamic model, in which various kinds of equations of state (EoS) with latent heats are considered, successfully explained the elliptic flow v_2 at transverse momentum $p_t < 2\mathrm{GeV}/c$ at RHIC energies [13, 14, 15]. However, hydrodynamics failed to explain the experimental R_O/R_S data ([8] and the references therein), i.e. the ratio between the HBT radii in outward and sideward directions, where the "t-puzzle" initially occurred. But recently, it has been realized that a direct (fully "apple-to-apple") comparison between hydro calculations and data is required [16].

In the transport models, the effective EoS is softened by the existence of resonances, but the re-scattering between particles will reinforce to some extent the stiffness of the dense matter. At SPS and RHIC energies, the color-string excitation and fragmentation is further considered for particle production and subsequent evolution in the ultra-relativistic/relativistic quantum molecular dynamics (UrQMD/RQMD) hadron-string transport models. The formation time of the hadrons from string fragmentation is determined by a "yo-yo" mode [17, 18]. During the formation time, the "pre-formed" particles (string fragments that will be projected onto hadron states later on) are usually treated to be free-streaming, while reduced cross sections are only included for leading hadrons. The idea of "pre-formed" hadrons is a well-

*E-mail address: liqf@fias.uni-frankfurt.de

known concept in the description of deep inelastic scattering data (DIS) [19, 20]. It has also been found that the "pre-formed" hadrons from the color fluxtube fragmentation behave already very hadronlike, before the hadron formation is fully completed [21]. In previous calculations [17, 18, 22], the interaction of the newly created "pre-formed" particles from the string fragmentation is usually not taken into account for simplicity. The facts have shown that the effective EoS at the early stage in the past model simulations is too soft and the early pressure is inadequate to match the calculated elliptic flow to the experimentally observed flows at RHIC energies [23, 24]. In order to make up for this discrepancy in the early-stage EoS, it is essential to modify the dynamics of the early stage with/without new degrees of freedom, such as done in a multi-phase transport (AMPT) [11], the hadronic rescattering (HRM) [25], the quark molecular dynamics (qMD) [26], and the parton hadron string dynamics (PHSD) [27] model.

Besides the new matter which is dominant at the early stage, the potentials between confined hadrons which play a role during almost all time of the collision process deserve attention as well. In the previously low energy UrQMD calculations, the Hamiltonian H served for the EoS consists of the kinetic energy T and the effective two-body interaction potential energy U. The potential energy U is indispensable, which includes the two-body and three-body (which can be approximately written in the form of two-body interaction) Skyrme- (also called as the density dependent terms), Yukawa-, and Coulomb-terms [17, 18]. Recently, in order to be more successfully applied in the intermediate energy region ($E_b \lesssim$ 2A GeV), more terms are considered [28, 29], those are, the density-dependent symmetry potential (essential for isospin-asymmetric reactions at intermediate and low energies) and the momentum-dependent term. At higher energies, i.e., AGS/FAIR and SPS, the Yukawa- and symmetry- potentials of baryons becomes negligible, while the Skyrme- and the momentum-dependent part of potentials still influence the whole dynamic process of HICs though weakly. In Ref. [30], the effects of the mean field with momentum dependence on collective flows from HICs at 2-158A GeV energies were studied by a Jet AA Microscopic Transportation Model (JAM) and it has been found that the momentum dependence in the nuclear mean field is important for the understanding of the proton collective flows at AGS and even at SPS energies. Further, by adopting the same soft EoS with momentum dependence (SM-EoS) on confined baryons, we also found that the calculated R_O/R_S ratio from HICs at AGS energies can be vastly improved when compared to the measured data [12, 31].

In this work, we will follow this idea and investigate the HBT radii at higher beam energies, i.e. SPS and RHIC. Furthermore, the other observables, such as the rapidity distributions of net protons ($p-\bar{p}$) and pions, and the elliptic flows of charged hadrons, are checked at the same time. As an initial attempt, we consider potentials for both formed and "pre-formed" particles: 1), for formed baryons, the SM-EoS [30] is chosen. The Coulomb potential is also considered, as in the low-energy calculations [28, 31]. 2), for formed mesons, only the Coulomb potential is optional in calculations, while other potentials are not considered as in previous calculations at low energies [28, 31]. 3), for "pre-formed" particles from string fragmentation, the similar density dependent (Skyrme-like) terms [49] as the formed baryons are used, but without the Yukawa, the Coulomb, and the momentum dependent terms. 4), the "pre-formed" mesons act like "pre-formed" baryons but with a reduction factor (2/3) due to the quark-number difference. Furthermore, 5), there is no potential interaction between "pre-formed" baryons and formed baryons so far. Correspondingly, the hadronic density is calculated by $\rho_h = \sum_{j\neq i} c_i c_j \rho_{ij}$, where $c_{i,j} = 1$ for Baryons, 2/3 for "pre-formed" mesons, and 0 for formed mesons. ρ_{ij} is a Gaussian in coordinate space. As stated in [30, 31], the relativistic effect (Lorentz transformation) on the relative distance and relative momentum between two particles i and j has been considered.

To set the stage, Fig. 1 shows the rapidity dependence of the multiplicities of net protons (top) and negatively charged pions (bottom) for central ($< 5\%$ of total cross section σ_T) Pb+Pb collisions at E_b = 158A GeV. The experimental data (solid stars) are taken from [32, 33], and the open stars represent the data reflected at mid-rapidity. The dash-dot-dotted lines are the cascade mode calculations, the dashed lines represent the calculations with SM-EoS of confined baryons, while the solid lines illustrate the results with the additional density-dependent potentials for "pre-formed" particles. While the cascade calculations give a reasonable rapidity distribution for the pions, the rapidity distribution of net protons is Gaussian - as seen in previous UrQMD calculations [22], and not fully consistent with the data (which has a two-bump structure at $y \sim \pm 1.2$). After considering the baryonic potentials, the distribution only changes slightly at projectile and target rapidities. However, when the density-dependent EoS for "pre-formed" particles is additionally taken into account, one observes that two bumps in the rapidity distribution of net protons appear. This implies that, due to the interactions of "pre-formed" particles at early stage, the additional pressure increases the effective stopping power as well as the central density at the compression stage. The total pion multiplicity remains basically unchanged on a level below 5% at this beam energy. Thus, the current pion distribution with potentials is acceptable for further investigations.

Using the analyzing program "correlation afterburner" (CRAB v3.0β), which is contributed by S. Pratt [34, 35], we calculate the HBT correlator and further fit it as a three-dimensional Gaussian form under the Pratt convention, i.e., the longitudinally comoving system (LCMS), which is expressed as

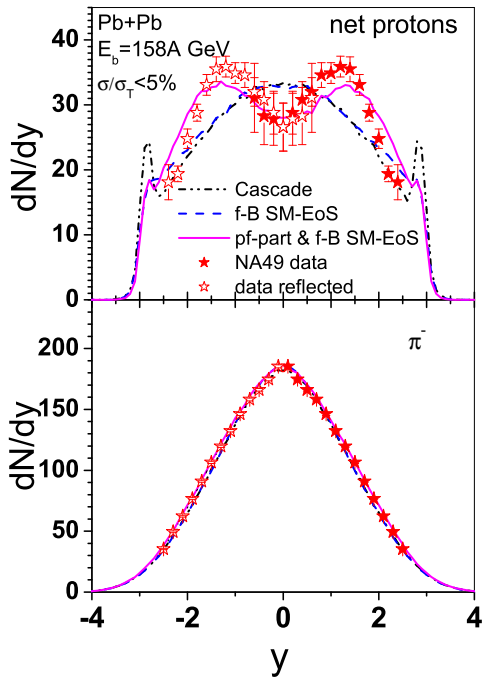

FIG. 1: Rapidity distributions of net protons (top) and negatively charged pions (bottom) from central ($< 5\%$ of total cross section) Pb+Pb collisions at $E_b = 158$A GeV. The experimental data (solid stars) are taken from [32, 33], while the open stars represent the data reflected at $y = 0$ in the center-of-mass system. The dash-dot-dotted lines are the calculations with cascade mode, the dashed lines represent the calculations with potentials for confined baryons (SM-EoS), while in the solid lines, the density-dependent potentials for "pre-formed" particles are further taken into account.

$$C(q_O, q_S, q_L) = 1+\lambda\exp(-R_L^2 q_L^2 - R_O^2 q_O^2 - R_S^2 q_S^2 - 2R_{OL}^2 q_O q_L). \quad (1)$$

In Eq. (1) the λ is the incoherence factor, R_L, R_O, and R_S are the Pratt radii in longitudinal, outward, and sideward directions, while the cross-term R_{OL} plays a role at large rapidities. q_i is the pair relative momentum in the i direction. Fig. 2 shows the transverse momentum k_T dependence ($\mathbf{k}_T = (\mathbf{p}_{1T} + \mathbf{p}_{2T})/2$) of the HBT-radii R_L, R_O, and R_S (at midrapidity) for central HICs at AGS (E_b = 2A, 4A, 6A, and 8A GeV), SPS (E_b = 20A, 30A, 40A, 80A, and 158A GeV), and RHIC ($\sqrt{s_{NN}} = 130$ and 200 GeV) energies. The physical cuts used are same as those listed in [12]. The data are from the E895, NA49, STAR, and PHENIX collaborations [36, 37, 38, 39, 40, 41]. The calculations with cascade mode are shown by lines with down-triangles while the calculations with various potential treatments are shown with other lines with different symbols. At $E_b = 2$A GeV, we show a comparison of calculations between with and without Coulomb potentials for confined mesons. It is seen that the two-body mesonic Coulomb potential before freeze-out affects the HBT radii only very weakly at about $k_T < 100$MeV/c, and the ratio between R_O and R_S values is not altered consequently. At AGS energies, besides the nuclear potentials, the Coulomb potential of confined mesons is also considered (solid lines with circles), while at SPS and RHIC energies, the Coulomb potential for confined mesons is switched off in order to save computing times and to avoid problems with non-local interactions. It is known that, below AGS energies hadrons are dominantly produced from the decay of resonances so that the considered potentials for "pre-formed" particles from string fragmentations have no effect on the HBT radii [42, 43]. At higher energies "pre-formed" particles play a dominant role for the early stage dynamics, which can be seen, e.g., by the comparison of solid lines and the lines with triangles at $\sqrt{s_{NN}} = 200$ GeV. So far the question of a steeper k_T-dependence of HBT radii than data at high SPS and RHIC energies, similar to the AMPT transport model calculations with parton scatterings [11], is still open.

The most exciting results show up in the transverse space. Roughly speaking, the nuclear potentials lead to a smaller R_O (especially at large k_T) but a larger R_S (especially at small k_T) generally allowing for a better description of the k_T dependent data. Certainly, our present crude approach is only semi-realistic as a description of the dynamic processes at the early stage of the reaction. However, one can still come to the conclusion that the potentials help to obtain a better description of the pion freeze-out in the transverse space.

In Fig. 3 we depict the excitation function of the R_O/R_S ratio at small k_T: at AGS and SPS energies, the results at k_T 150 ± 50MeV/c are shown, while at RHIC energies, the k_T is set to 200 ± 50MeV/c. The experimental data within the transverse momentum regions are compared with the calculations with and without potentials. As seen before [12, 44, 45], in the cascade mode (dash-dot-dotted lines with open rectangles) the R_O/R_S ratio, which is related to the duration of the emission τ ($\tau \sim \sqrt{R_O^2 - R_S^2}$), is larger than the experimentally observed values at all investigated energies. Furthermore, the increase of the R_O/R_S ratio with beam energies at AGS is not seen in these calculations. When the SM-EoS is considered for confined baryons (dashed lines with open up-triangles), the R_O/R_S ratio decreases compared to the result in the cascade mode and reproduces the energy dependence of the data up to the lower SPS energies. At high SPS and RHIC energies, however, the R_O/R_S ratio increases further with increasing beam energies and deviates strongly from the data at top RHIC energies. Here, the ratio nearly approaches the value obtained in the cascade mode. It implies that the potential of confined hadrons is increasingly losing its importance with increasing beam energy. At SPS and RHIC energies the deviation from data can be interpreted by the absence of interactions of "pre-formed" particles from string fragmentation since at $E_b \sim 30 - 40$A GeV the measured R_O/R_S ratio begins to flatten/decrease in contrast to

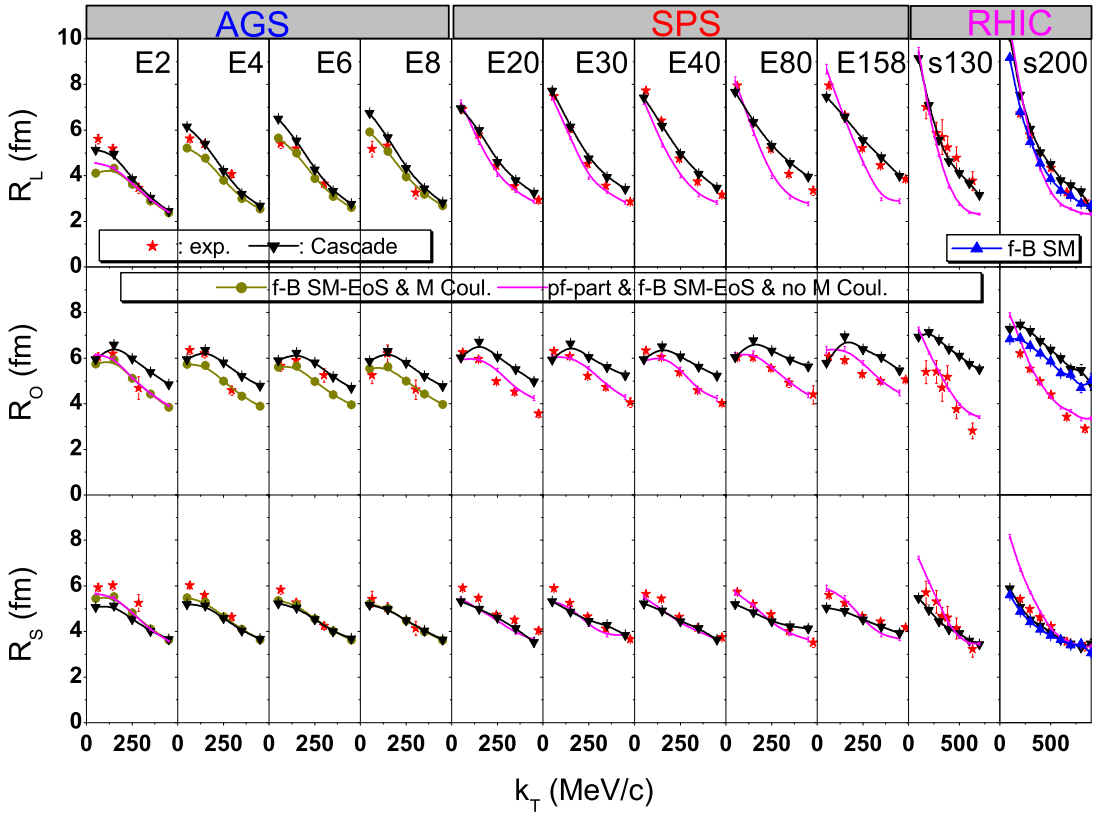

FIG. 2: Transverse momentum k_T dependence of the HBT radii R_L, R_O, and R_S (at midrapidity) for central HICs at AGS (E_b = 2A, 4A, 6A, and 8A GeV), SPS (E_b = 20A, 30A, 40A, 80A, and 158A GeV), and RHIC ($\sqrt{s_{NN}}$ = 130 and 200 GeV) energies. The data are indicated by solid stars, which are from E895, NA49, STAR, and PHENIX collaborations [36, 37, 38, 39, 40, 41]. The calculations with cascade mode are shown by lines with down-triangles. At AGS energies, the calculations with potentials for confined baryons (SM-EoS) as well as a Coulomb potential for confined mesons are shown by the lines with circles. At AGS E_b = 2A GeV, SPS, and RHIC energies, the results with potentials for both "pre-formed" particles and confined baryons but without Coulomb potential for mesons are shown by lines, while the lines with up-triangles correspond to the calculations without any potentials for "pre-formed" particles but with potentials for confined baryons.

the aforementioned calculations. However, with the consideration of a density dependent EoS for "pre-formed" hadrons (solid lines with open down-triangles) this behavior can be reproduced in the calculations. With this approach, at RHIC energies, the ratio R_O/R_S is about unity (slightly below data) which implies that the compressibility provided by the currently employed potential is too strong. Nevertheless, since we are not aiming at fitting the whole excitation function of the data, we leave this detail aside for further detailed explorations.

Therefore, our explanation of the HBT time related puzzle is different from the investigations in Ref. [46] where Cramer, et al., considered a single-pion optical potential which simulates its interactions with the dense medium. While in this work, the microscopic "nuclear" potentials are considered for "pre-formed" hadrons from the string fragmentation. The Hamilton's equations of motion of the particles represented by Gaussian wave packets are solved microscopically. After that, the freeze-out phase space is analyzed numerically by the CRAB program, in which the plain and distorted (by Coulomb and nuclear potentials after freeze-out) wave functions are optional.

Let us finally check the modification of the early transverse expansion by a look into the elliptic flow. In the upper plots of Fig. 4 we present the transverse momentum p_t dependence of the elliptic flow v_2 ($v_2 = \langle(p_x^2 - p_y^2)/p_t^2\rangle$, where $p_t^2 = p_x^2 + p_y^2$) of charged pions from Au+Au collisions at RHIC $\sqrt{s_{NN}}$ = 200 GeV. Two sets of centralities are chosen: $5\% < \sigma/\sigma_T < 10\%$ (in (a)) and $20\% < \sigma/\sigma_T < 30\%$ ((b)). To avoid non-flow effects [47], the four-particle integral cumulant v_2 data ($v_2\{4\}$) are shown with stars. Similar to those in Fig. 3, the UrQMD calculations without and with potentials are illustrated

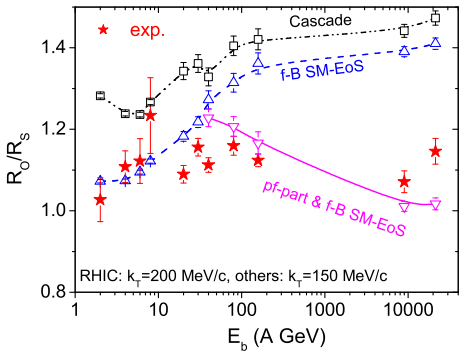

FIG. 3: Excitation function of the R_O/R_S ratio at small k_T. The data are indicated by solid stars. The dash-dot-dotted lines with open rectangles are results under cascade mode, the dashed lines with open up-triangles represent the calculations with potentials for confined baryons, while the solid lines with open down-triangles are results with potentials for both "pre-formed" and confined particles.

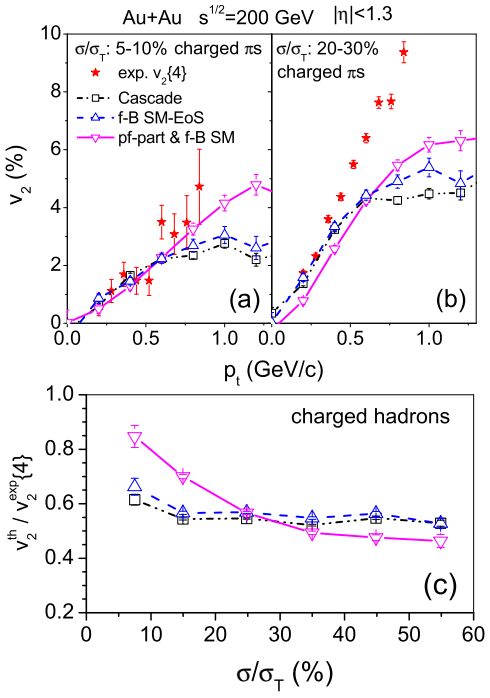

FIG. 4: Top plots ((a) and (b)): Transverse momentum p_t dependence of the elliptic flow v_2 for Au+Au collisions at RHIC $\sqrt{s_{NN}} = 200$ GeV. The pseudo-rapidity cut is $|\eta| < 1.3$. Two sets of centralities are chosen: $5\% < \sigma/\sigma_T < 10\%$ (in (a)) and $20\% < \sigma/\sigma_T < 30\%$ ((b)). Stars represent the four-particle integral cumulant v_2 data ($v_2\{4\}$). Dash-dot-dotted lines with open rectangles represent the cascade calculations. Dashed lines with open up-triangles are the results with confined baryonic potentials, while the solid lines with open down-triangles are the results with potentials for both "pre-formed" particles and confined baryons. Bottom plot ((c)): Centrality dependence of the ratio between theoretical and experimental flows of charged hadrons, which are integrated over p_t and η.

for comparison with data. It is clear that due to the absence of early pressure, the elliptic flow in the cascade mode (dash-dot-dotted lines with open rectangles) can not grow as fast as the data with the increase of transverse momentum in both centralities. After switching on the SM-EoS for confined baryons (dashed lines with open up-triangles), the flow is seen to increase slightly especially at high transverse momenta. With the density dependent potentials for "pre-formed" particles (solid lines with open down-triangles), the elliptic flow at large transverse momenta rises further, however, at small transverse momenta it is driven down and deviates from data especially at large centralities. This phenomenon calls for a more complete description of the dynamics of HICs at high energies in which the (in)elastic scatterings of particles (confined hadrons and deconfined partons) should be considered in more detail. To make a whole comparison, we show in Fig. 4 (c) the centrality dependence of the ratio between different theoretical v_2 values of charged hadrons and the four-particle cumulant data ("$v_2^{th}/v_2^{exp}\{4\}$", here the flows are integrated over p_t and η). As stated before, the flow obtained from the cascade calculation is only about 55% of the experimental one. The contribution of potentials of confined baryons to flow is only at the level of about 4%. While the potentials of "pre-formed" hadrons increase the flow in more central collisions. At large centrality, the potential effects are relatively weak.

In summary, besides a soft equation of state with momentum dependence, which is required especially at low energies, a density dependent (Skyrme-like) potential has been tested for the "pre-formed" particles from string fragmentation in the UrQMD transport model. Although the form of the potential for the new phase is simple and rough (ideally, the EoS of the new phase should be based on the first-principle lattice QCD calculations [48]), it provides new insights into the dynamics of HICs. It reproduces the proper stopping power for net protons. It also improves the elliptic flow at large transverse momenta. Most importantly however, it decreases the HBT radius R_O but increases the R_S so that the experimental duration time related quantity — here the R_O/R_S ratio — can be reasonably reproduced throughout the energies from AGS, SPS, up to RHIC. Although some open problems remain due to the simple treatment of the interaction of the particles at the early stage.

Acknowledgements

We would like to thank S. Pratt for providing the CRAB program and acknowledge support by the Frankfurt Center for Scientific Computing (CSC). We also

thank M Gyulassy, H J Drescher, and S Haussler for helpful discussions. Q. Li thanks the Frankfurt Institute for Advanced Studies (FIAS) for financial support. This work is partly supported by GSI, BMBF, and Volkswagenstiftung.

[1] T. D. Lee, Nucl. Phys. A **750** (2005) 1.
[2] M. Gyulassy and L. McLerran, Nucl. Phys. A **750** (2005) 30.
[3] E. V. Shuryak, Nucl. Phys. A **750** (2005) 64.
[4] L. M. Satarov, H. Stoecker and I. N. Mishustin, Phys. Lett. B **627** (2005) 64.
[5] R. A. Janik and R. Peschanski, Phys. Rev. D **73** (2006) 045013.
[6] T. Hirano and M. Gyulassy, Nucl. Phys. A **769** (2006) 71.
[7] D. H. Rischke and M. Gyulassy, Nucl. Phys. A **608** (1996) 479.
[8] M. A. Lisa, S. Pratt, R. Soltz and U. Wiedemann, Ann. Rev. Nucl. Part. Sci. **55** (2005) 357.
[9] P. Chung and P. Danielewicz [NA49 Collaboration], arXiv:0707.2690 [nucl-ex].
[10] P. Danielewicz and S. Pratt, Phys. Rev. C **75** (2007) 034907.
[11] Z. Lin, C. M. Ko and S. Pal, Phys. Rev. Lett. **89** (2002) 152301.
[12] Q. Li, M. Bleicher and H. Stoecker, J. Phys. G **34** (2007) 2037.
[13] P. Huovinen, arXiv:nucl-th/0305064.
[14] P. F. Kolb and U. W. Heinz, arXiv:nucl-th/0305084.
[15] P. Huovinen, Nucl. Phys. A **761** (2005) 296.
[16] E. Frodermann, U. Heinz and M. A. Lisa, Phys. Rev. C **73** (2006) 044908.
[17] S. A. Bass *et al.*, [UrQMD-Collaboration], Prog. Part. Nucl. Phys. **41** (1998) 255.
[18] M. Bleicher *et al.*, [UrQMD-Collaboration], J. Phys. G: Nucl. Part. Phys. **25** (1999) 1859.
[19] J. Czyzewski, Acta Phys. Polon. B **21** (1990) 41.
[20] A. Accardi, V. Muccifora and H. J. Pirner, Nucl. Phys. A **720** (2003) 131 ; W. Cassing, K. Gallmeister and C. Greiner, Nucl. Phys. A **735** (2004) 277 ; F. Arleo, Eur. Phys. J. C **30** (2003) 213 ; B. Z. Kopeliovich, J. Nemchik and I. Schmidt, Nucl. Phys. A **782** (2007) 224.
[21] A. Bialas and M. Gyulassy, Nucl. Phys. B **291**, 793 (1987) ; A. Bialas and J. Czyzewski, Phys. Lett. B **222**, 132 (1989).
[22] E. L. Bratkovskaya *et al.*, Phys. Rev. C **69** (2004) 054907.
[23] X. Zhu, M. Bleicher and H. Stoecker, Phys. Rev. C **72** (2005) 064911.
[24] M. Bleicher and H. Stoecker, Phys. Lett. B **526** (2002) 309.
[25] T. J. Humanic, Int. J. Mod. Phys. E **15** (2006) 197.
[26] M. Hofmann, M. Bleicher, S. Scherer, L. Neise, H. Stoecker and W. Greiner, Phys. Lett. B **478** (2000) 161 ; S. Haussler, S. Scherer and M. Bleicher, arXiv:hep-ph/0702188.
[27] I. C. Arsene *et al.*, Phys. Rev. C **75** (2007) 034902 ; W. Cassing, arXiv:0707.3033 [nucl-th].
[28] Q. Li, Z. Li, S. Soff, M. Bleicher and H. Stoecker, J. Phys. G **32** (2006) 151.
[29] B. A. Li, C. B. Das, S. D. Gupta and C. Gale, Phys. Rev. C **69** (2004) 011603.
[30] M. Isse, A. Ohnishi, N. Otuka, P. K. Sahu and Y. Nara, Phys. Rev. C **72** (2005) 064908.
[31] Q. Li, M. Bleicher, and H. Stöcker, in preparation.
[32] S. V. Afanasiev *et al.* [The NA49 Collaboration], Phys. Rev. C **66** (2002) 054902.
[33] H. Appelshauser *et al.* [NA49 Collaboration], Phys. Rev. Lett. **82** (1999) 2471.
[34] S. Pratt *et al.*, Nucl. Phys. A **566** (1994) 103C.
[35] S. Pratt, CRAB version 3, http://curly.pa.msu.edu/∼scottepratt/freecodes/crab/home.html
[36] M. A. Lisa *et al.* [E895 Collaboration], Phys. Rev. Lett. **84** (2000) 2798.
[37] S. Kniege *et al.* [NA49 Collaboration], AIP Conf. Proc. **828** (2006) 473.
[38] C. Adler *et al.* [STAR Collaboration], Phys. Rev. Lett. **87** (2001) 082301.
[39] J. Adams *et al.* [STAR Collaboration], Phys. Rev. C **71** (2005) 044906.
[40] S. S. Adler *et al.* [PHENIX Collaboration], Phys. Rev. Lett. **93** (2004) 152302.
[41] K. Adcox *et al.* [PHENIX Collaboration], Phys. Rev. Lett. **88** (2002) 192302.
[42] H. Weber *et al.*, Phys. Lett. B **442** (1998) 443. [arXiv:nucl-th/9808021].
[43] H. Petersen and M. Bleicher, PoS **CPOD2006** (2006) 025.
[44] Q. Li, M. Bleicher and H. Stoecker, Phys. Rev. C **73** (2006) 064908.
[45] Q. Li, M. Bleicher, X. Zhu and H. Stoecker, J. Phys. G **33** (2007) 537.
[46] J. G. Cramer, G. A. Miller, J. M. S. Wu and J. H. S. Yoon, Phys. Rev. Lett. **94** (2005) 102302 [Erratum-*ibid.* **95** (2005)] 139901.
[47] J. Adams *et al.* [STAR Collaboration], Phys. Rev. C **72** (2005) 014904.
[48] M. Bluhm, B. Kampfer, R. Schulze, D. Seipt and U. Heinz, arXiv:0705.0397 [hep-ph].
[49] $U(\rho_h/\rho_0) = \alpha(\rho_h/\rho_0) + \beta(\rho_h/\rho_0)^\gamma$, where ρ_h is the hadronic density, $\rho_0 = 0.16fm^{-3}$ is the normal nuclear density. α, β, and γ are parameters, in this work for the SM-EoS, they are, -268 MeV, 345 MeV, and 7/6, respectively.